

Internal vs Forced Variability Metrics for Geophysical Flows Using Information Theory

Aakash Sane^{1,1}, Baylor Fox-Kemper^{1,1,1}, David Ullman^{2,2,2}, and Aakash Sane¹

¹Brown University

²University of Rhode Island

August 10, 2023

Abstract

We demonstrate the use of information theory metrics, Shannon entropy and mutual information, for measuring internal and forced variability in general circulation coastal and global ocean models. These metrics have been applied on spatially and temporally averaged data. A combined metric reliably delineates intrinsic and extrinsic variability in a wider range of circumstances than previous approaches based on variance ratios that therefore assume Gaussian distributions. Shannon entropy and mutual information manage correlated fields, apply to any distribution, and are insensitive to outliers and a change of units or scale. Different metrics are used to quantify internal vs forced variability in (1) idealized Gaussian and uniformly distributed data, (2) an initial condition ensemble of a realistic coastal ocean model (OSOM), (3) the GFDL-ESM2M climate model large ensemble. A metric based on information theory partly agrees with the traditional variance-based metric and identifies regions where non-linear correlations might exist. Mutual information and Shannon entropy are used to quantify the impact of different boundary forcings in a coastal ocean model ensemble. Information theory enables ranking the potential impacts of improving boundary and forcing conditions across multiple predicted variables with different dimensions. The climate model ensemble application shows how information theory metrics are robust even in a highly skewed probability distribution (Arctic sea surface temperature) resulting from sharply non-linear behavior (freezing point).

1 **Internal vs Forced Variability Metrics for General**
2 **Circulation Models Using Information Theory**

3 **Aakash Sane^{1*}, Baylor Fox-Kemper², and David S. Ullman³**

4 ¹School of Engineering, Brown University, Providence, Rhode Island, USA

5 ²Department of Earth, Environment, and Planetary Sciences, Brown University, Providence, Rhode
6 Island, USA

7 ³Graduate School of Oceanography, University of Rhode Island, Narragansett, Rhode Island, USA

*Aakash Sane's current affiliation: Atmospheric and Oceanic Sciences, Princeton University, Princeton, New Jersey

Corresponding author: Aakash Sane, aakash.sane@princeton.edu

Abstract

Ocean model simulations show variability due to intrinsic chaos and external forcing (air-sea fluxes, river input, anthropogenic emissions, etc.). It is important to estimate their contributions to total variability for attribution. Using variance to estimate variability might be unreliable due to the existence of higher statistical moments. We show the use of non-parametric information theory metrics, Shannon entropy and mutual information, for measuring internal and forced variability in coastal and global ocean models. These metrics are applied on spatially and temporally averaged data. Metrics delineate variability in a wider range of circumstances than previous approaches based on variance ratios that assume Gaussian distributions. Metrics work on correlated fields, apply to any distribution, and are insensitive to outliers and a change of units or scale. Metrics are applied to (1) idealized data, (2) ensemble of a realistic coastal ocean model (OSOM), (3) GFDL-ESM2M large ensemble. The information theory metric partly agrees with the variance-based metric and possibly identifies regions of non-linear correlations. The metric detects higher intrinsic variability in the Arctic region as compared to the variance metric. The climate model ensemble application shows how information theory metrics are robust in a skewed probability distribution (Arctic sea surface temperature) resulting from sharply non-linear behavior (freezing point). In different experiments, we quantify sensitivity of OSOM to changes in forcing. Variations in the river runoff and changing the wind product do not add information (variability). Information theory enables ranking the impacts of improving boundary and forcing conditions across multiple variables with different dimensions.

Plain Language Summary

It is important in climate modeling to distinguish variability caused by external forces versus variability that arises within the system to estimate causes in a particular variation. Disturbances from the atmosphere such as wind, solar heating and cooling, anthropogenic emissions are external disturbances and variations due to swirls are internal chaotic disturbances. We use information theory - a way to quantify the amount of variability in these models. Here, we study multiple runs of a coastal ocean model and an ocean climate model. We found that it matters a lot how you measure the internal and external variability. Making fewer assumptions about the statistics of variability proved more robust, especially in the Arctic in global model and at depth in an estuary. For the global model, we found internal chaos to dominate temperature variations in the Arctic in contrast to variations in salinity. In a different set of experiments, the coastal model was run by slightly changing the wind, averaging the river input instead of the full river flow, etc. We found that we cannot neglect river input. Different winds had the same impact. These experiments reveal the importance of uncertainty in forcing conditions to help us design a forecasting system.

1 Introduction

In an ocean or climate model, it is pertinent to understand the cause of variability, as it leads to implications for predictability, prioritization of data collections for assimilation, and provides an understanding of the dynamics at play in different regions. In a coastal model, variability can arise from extrinsic factors such as wind forcing, solar and thermal forcing, tides, rivers, evaporation, and precipitation, or it can be due to internal chaos inherent to the governing fluid equations (Sane et al., 2021). In a climate model, modes of variability such as El Niño, the North Atlantic Oscillation, or the Southern Annular Mode can conceal or delay the emergence of attributable anthropogenic climate change signals (Milinski et al., 2019). In high-resolution ocean models, internal chaos or intrinsic variability can also be due to eddies (Leroux et al., 2018; Llovel et al., 2018). Accurately quantifying the relative contribution of external

58 and internal factors can help to elucidate the causes responsible for observed variability
 59 in models, help to identify key observable metrics, and help quantify concepts such
 60 as the time of emergence of climate signals (Hawkins & Sutton, 2012).

61 Numerous methods exist in the literature to quantify intrinsic and extrinsic variability
 62 using models or observations (e.g., Frankcombe et al. (2015); Schurer et al.
 63 (2013); Y.-C. Liang et al. (2020)). Two types of model ensembles are common: initial
 64 condition ensembles (where the same model is used repeatedly with perturbed initial
 65 conditions and intrinsic variability occurs via chaos), and multi-model ensembles
 66 (where a variety of models differing in numerics and parameterizations are used to simulate
 67 change under the same forcing—in this case “intrinsic” variability also includes
 68 aspects of model formulations). Initial condition ensembles are a set of simulations
 69 sharing the same forcing and the same governing equations and identical parameterizations,
 70 but they still diverge from one another because slightly different initial
 71 conditions evolve into substantially different conditions later in the simulations due to
 72 intrinsic chaos—most geophysical fluid dynamics models and climate models are intrinsically
 73 chaotic. Most of the discussion here will focus on initial condition ensembles,
 74 but the metrics proposed can be adapted to both types of ensembles.

75 To help visualize variability, a generic idealized output from an ocean or atmospheric
 76 model is shown in Figure 1. Each color represents a different ensemble member,
 77 and the black solid line is the mean of those members. The solid black line is the signal
 78 due mainly to extrinsic factors (aside from the limits of the finite ensemble size)
 79 and the spread of the model (schematized by the double-headed magenta arrow in
 80 Figure 1) can be considered due to intrinsic variability or internal chaos.

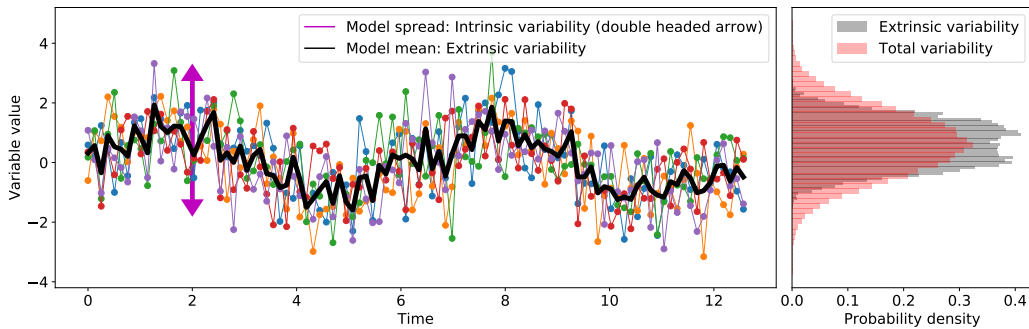


Figure 1. A sketch of a typical ocean or climate model output for an arbitrary variable. Each ensemble is shown in a different color, and the mean of the ensemble is shown as a black line. The ensemble mean can be considered to be the trend set by external forcings. The model spread shown by the double-headed magenta arrow indicates the chaos of the model.

81 One method of quantifying intrinsic and extrinsic variability is to look at vari-
 82 ances (second central statistical moment) of the model spread and the mean of the
 83 model (Leroux et al., 2018; Lovel et al., 2018; Waldman et al., 2018; Yettella et al.,
 84 2018). Variance is sufficient to constrain all metrics of variability about the mean when
 85 distributions are Gaussian and uncorrelated, but a single statistical moment usually
 86 measures only part of a more complex variability distribution. Many climatological
 87 variables show non-Gaussian distributions (e.g., Franzke et al. (2020)). In fact, gener-
 88 alized variance might be misleading (e.g., Kowal (1971)). Quantification of variability
 89 should be robust to or have a known dependence on changes in the units of the quan-
 90 tity or the scale (e.g., changing temperature from Celsius to Fahrenheit or Kelvin).

91 Comparative metrics, such as intrinsic vs. extrinsic variability, should not depend on
92 these arbitrary choices of units at all.

93 Variability, in essence, is a function of the number of occurrences or frequency
94 of occurrence, often estimated by a histogram formed after appropriately binning the
95 data, which then approximates a distribution with a discrete probability p_i as a fraction
96 over all states of the visited system. A histogram thus makes the estimated and
97 visited number of states discrete rather than continuous. Information entropy metrics
98 measure variability by taking into account the probability distribution of the binned
99 data, drawing on the concept from statistical mechanics of entropy in quantifying
100 the number of microstates that a variable can occupy. The fundamental measure in
101 information theory is the Shannon entropy (Shannon, 1948) (a.k.a. the information
102 entropy) that characterizes the amount of variability in a variable (Carcassi et al.,
103 2021). Mutual information, another metric introduced by Shannon (1948), measures
104 how much information a variable contains about another variable.

105 Information theory is applied in signal processing, computer science, statistical
106 mechanics, quantum mechanics, etc. It is used to quantify the amount of informa-
107 tion, disorder, freedom, or lack of freedom (Brissaud, 2005). The application of these
108 abstract notions to geophysical flows can have immense practical benefit when infor-
109 mation entropy is interpreted as a measure of variability, as entropy does not rely on
110 any particular parametric probability distribution. Information theory metrics are not
111 new to climate sciences. They have been introduced in predictability studies, evalu-
112 ating the skill of statistical models, as well as uncertainty studies (Leung & North,
113 1990; Schneider & Griffies, 1999; Kleeman, 2002; DelSole & Tippett, 2007; Majda &
114 Gershgorin, 2010; Stevenson et al., 2013) and recently in studying variability (Gomez,
115 2020), coastal predictability (Sane et al., 2021) and drivers of drought (Shin et al.,
116 2023).

117 In the two parts of this article, we bring well-established concepts of information
118 theory to the particular application of measuring intrinsic and extrinsic variability
119 for ensemble model runs within atmospheric and oceanographic modeling. We use
120 Shannon entropy and mutual information and a particularly useful combination of the
121 two. We indirectly employ conditional entropy, which depends on Shannon entropy
122 and mutual information but is less intuitive so is not discussed in detail. Recent theo-
123 retical advances in understanding dynamical systems through the lens of information
124 theory relate causality analysis and information transfer (e.g., X. S. Liang (2014)).
125 Although important, this theory has had few concrete applications. Even the basic
126 information theory concepts (Shannon entropy and mutual information) have enjoyed
127 only limited adoption by the oceanic and atmospheric community, primarily arising
128 in predictability quantification (e.g., Sane et al. (2021)). We begin to bridge the gap
129 with a pragmatic framework which can be easily replicated and improved upon, in-
130 cluding causality analysis and the evolution of entropy within modeling systems like
131 those studied here.

132 In Part 1, we apply this intrinsic vs. extrinsic metric to three sets of data: 1)
133 Idealized Gaussian and uniformly distributed arrays with specified correlation, 2)
134 Initial condition ensemble output of a regional coastal model (OSOM) (Sane et al., 2021)
135 over July-August 2006 where most variables are not Gaussian, and 3) The GFDL-
136 ESM2M Large Ensemble (Rodgers et al., 2015; Deser et al., 2020), an climate model
137 initial condition ensemble hereby referred to as GFDL-LE. This large ensemble dataset
138 contains historical and future projection data following the RCP 8.5 scenario. All the
139 GFDL-LE monthly mean data from 1950 to 2100 were used in the analysis.

140 In Part 2, we use OSOM to demonstrate the use of Shannon entropy and mutual
141 information to quantify the extrinsic forcing effects of altered boundary forcing types.
142 For example, is wind forcing dominant over river forcing, does using temporal averaged
143 river runoff cause any appreciable changes in estuarine circulation, or does change in

144 the wind product alter circulation? In coastal and estuarine systems, knowledge of
 145 which forcings are dominant helps prioritize data collection and refinement of the
 146 most impactful forcings.

147 1.1 Information theory

148 We introduce information theory concisely assuming the reader has no back-
 149 ground knowledge—this section contains standard definitions. Consider a probability
 150 distribution p_i obtained after binning data into N bins. The user chooses the appro-
 151 priate number of bins or bin widths for the range of data. Shannon (1948) identified
 152 the average information content in N possible outcomes, equally or not equally likely,
 153 as given by:

$$H = \sum_{i=1}^N p_i \log_2(1/p_i), \quad (1)$$

154 where H is the Shannon entropy with unit of bits when log is base 2 and p_i is the
 155 probability of the i^{th} outcome. The factor $\log_2(1/p_i)$ measures the information of the
 156 i^{th} outcome as proposed by Hartley (1928) and is also a measure of uncertainty (Cover,
 157 1999), as it measures the information gained by knowing that the i^{th} outcome has
 158 happened or equivalently that the variable falls in the i^{th} bin. The term information
 159 does not mean knowledge, but it means the amount of uncertainty shown by a variable
 160 or the freedom that a variable has when visiting different combinations of the N bins.
 161 Shannon (1948) found Equation 1 to provide the average information (or uncertainty)
 162 for all events in a record. For the entire set of elements, a highly probable event has
 163 less uncertainty associated with it, and a low probability event has high uncertainty
 164 associated with it. Thus, the prefactor p_i is used to weight the information over all
 165 possibilities. One way to interpret the need for the prefactor p_i is that in repeated
 166 experiments the events with higher probability will occur more often; hence they should
 167 contribute more to the quantification of variability than infrequent events.

168 Stone (2015) gives an intuitive way to understand Shannon entropy using a binary
 169 tree. A binary tree is a tree chart which starts with one node and splits into two
 170 branches at each node. At each node you can take a left or right turn to proceed, and
 171 if there are, say, 3 levels in the tree, then 8 (i.e. 2^3) outcomes or possible destinations
 172 exist. If a binary tree has N equally probable outcomes, then the set of instructions
 173 required to reach the correct destination is given by $h = (N)(1/N) \log_2(N) = \log_2(N)$.
 174 The *uncertainty* about reaching the correct destination will be removed by providing
 175 $\log_2(N)$ bits of information. In other words, if the entropy is h then 2^h states are
 176 possible.

A second metric from Shannon (1948) which is also widely used is *mutual infor-*
mation. The mutual information between two signals x and y denoted by $I(X; Y)$ is
 (Cover, 1999)

$$I = \sum_{j=1}^N \sum_{i=1}^N p_{ij} \log_2 \left(\frac{p_{ij}}{p_i p_j} \right), \quad (2)$$

177 where p_{ij} is the joint probability of i^{th} outcome of x and j^{th} outcome of y . The marginal
 178 probability of i^{th} and j^{th} outcomes of x and y respectively are p_i and p_j . The addend
 179 within the summations can be expanded to $p_{ij} (\log_2(p_{ij}) - \log_2(p_i) - \log_2(p_j))$. I can
 180 be interpreted as the extra information in entropy of marginal distributions of x and y
 181 over the joint distribution. Mutual information is symmetric between x and y and is
 182 the measure of the amount of information they share. For example, if the distributions
 183 are statistically independent, then $p_{ij} = p_i p_j$ and thus $I = 0$. If the two records x
 184 and y are identical, then $p_{ij} = p_i = p_j$ and $I = H$. I is the average reduction in

185 uncertainty in x due to knowing y or vice versa and denotes how much information is
 186 transmitted between the two variables.

187 In the context of ocean or climate modeling, entropy can be used to measure vari-
 188 ability in a model output or available data. This is in tandem with the interpretation
 189 of Shannon entropy in physical sciences as given in Carcassi et al. (2021). When cal-
 190 culating the Shannon entropy, the primary concern is counting the possible states, e.g.
 191 the various bins in a histogram, where the variable can go into while any assigned bin
 192 value or its dimensions are of lesser importance. Entropy metrics measure variability
 193 in *bits* (when the logarithm is of base 2), and hence changing the scale, e.g. switching
 194 from Celsius to Fahrenheit for temperature, does not change the value of variability
 195 (under equivalent binning). Mutual information and entropy are both dimensionally
 196 agnostic. They are also not sensitive to outliers due to the weighting prefactor and
 197 can capture nonlinear interactions (Watanabe, 1960; Correa & Lindstrom, 2013) and
 198 discontinuous distributions, including states visited intermittently. We will present the
 199 effect of correlation and outliers by examples of idealized random vectors.

200 The following methods and results sections are divided into the two parts of the
 201 overall objective of the paper. Parts A of both sections relate to evaluating intrinsic
 202 and extrinsic variability in ensemble models. Parts B describe the usage of Shannon
 203 entropy and mutual information on coastal regional modeling data to understand and
 204 compare the effects of using different boundary conditions.

205 2 Methods

206 2.1 Part A: Intrinsic and Extrinsic Variability for Ensemble Data

Analysis begins on each grid point on the ocean surface or ocean bottom. Let
 a variable in the ensemble be given by $f(n, t, x, y)$ where f is the variable, n denotes
 the index of the ensemble member and goes from 1 to N , t is the time index and goes
 from t_1 to t_M , x, y represents the spatial grid point at the surface or bottom. The
 total number of members of the ensemble is N and each member has M time steps.
 At a particular grid point $f(n, t, x, y)$ is $f(n, t)$. To obtain the signal due to extrinsic
 forcings, the “differencing” approach (Frankcombe et al., 2015) has been followed to
 estimate the forced response. This approach involves averaging the members of the
 ensemble to derive *ensemble mean*. The ensemble mean is given by the following:

$$g(t) = \frac{1}{N} \sum_{n=1}^{n=N} f(n, t) \quad (3)$$

$g(t)$ is a single time-varying signal for each grid point obtained by averaging across the
 ensemble members. There are potential problems with assuming that the ensemble
 mean represents extrinsic variability only, such as if models are differently sensitive
 to the forcing signal based on the model’s equilibrium sensitivity, as elaborated in
 Frankcombe et al. (2015) and Johnson et al. (2023). For a first-order approximation,
 we will assume the ensemble mean is the best estimate of the forced response. Once
 $g(t)$ is obtained, the intrinsic variability can be estimated by subtracting the ensemble
 mean $g(t)$ from each ensemble member. The ensemble signal, forced response, and
 intrinsic variability are then related by:

$$f(n, t) = g(t) + \eta(n, t), \quad (4)$$

207 where $\eta(n, t)$ is the intrinsic variability or noise that differs from one ensemble member
 208 to another. Note that the above decomposition takes place at each grid point. In
 209 Figure 1a, $f(n, t)$ are shown by multi-colored ensemble members. $g(t)$ is shown by a
 210 thick black line. As seen in Figure 1b, $g(t)$ has a probability distribution shown in
 211 gray and subsequently has the first, second and possibly important higher statistical

212 moments. The gray density histogram shows variability due to extrinsic factors, and
 213 the pink density histogram shows total variability given by extrinsic and intrinsic
 214 factors.

215 **2.1.1 Evaluating entropies**

216 The ensemble simulation data has been used without detrending to evaluate $g(t)$
 217 and $\eta(n, t)$. Detrending will remove some nonstationarity from the data, but will also
 218 remove some part of the extrinsic variability. Our aim is not to determine the forced
 219 response but to estimate the degree of *variability* contributed by the forced response
 220 (extrinsic response) and the intrinsic variability originating from the intrinsic chaos.
 221 Metrics have been calculated at each grid point by treating them independently.

222 Usually we are limited in the number of ensemble members due to computational
 223 costs, so we concatenate into a *jugaad* in order to use *all* the ensemble members at
 224 once to evaluate information entropies. All the ensemble members given by $f(n, t)$ are
 225 rearranged into a single row vector f as:

$$f = [f(1, t_1), f(1, t_2), \dots, f(1, t_M), f(2, t_1), f(2, t_2), \dots, f(N - 1, t_M), f(N, t_1), \dots, f(N, t_M)], \quad (5)$$

226 and g is the row vector obtained by arranging N copies of $g(t)$ in the following fashion:

$$g = \underbrace{[g(t_1), g(t_2), \dots, g(t_M)]}_1, \underbrace{[g(t_1), g(t_2), \dots, g(t_M)]}_2, \dots, \underbrace{[g(t_1), g(t_2), \dots, g(t_M)]}_N \quad (6)$$

227 This enables wide sampling and obtains an accurate probability distribution for f (as-
 228 suming approximate stationarity, or enforcing stationarity by detrending), and allows
 229 g to be of the same size as f and having the same probability distribution as that of
 230 $g(t)$. The information statistics we get at each grid point are time-invariant, since the
 231 complete time series is considered. It is the user's choice to choose either the complete
 232 time series or a section of it for analysis. We have chosen the whole time series be-
 233 cause this is a sufficient demonstration of the value of information theory metrics. A
 234 time-evolving analysis raises additional issues about causality and the shifting proba-
 235 bilities distributions of climate states that are not the focus here (X. S. Liang, 2013;
 236 DelSole & Tippet, 2018). By using the whole time series, we treat all variability as
 237 drawn from the same distribution and seek only to associate internal (associated with
 238 each ensemble member) and external (associated with the ensemble mean) sources of
 239 variability following Leroux et al. (2018). The time series f and g are both expressed
 240 as row vectors of the same size, $N \times M$. This step is crucial, as vectors having the
 241 same number of elements are necessary to evaluate joint probability distribution. This
 242 enables us to calculate the mutual information between f and g .

243 Calculating the Shannon entropy of f and the mutual information between f
 244 and g is a difficult task that necessitates careful consideration. Optimal binning for
 245 precise measurement of information entropies is a research topic in itself, and vari-
 246 ous techniques have been proposed, such as equidistant partitioning, equiprobable
 247 partitioning, k nearest neighbor, usage of B-spline curves for binning to name a few
 248 (Hacine-Gharbi et al., 2012; Kowalski et al., 2012; Knuth, 2019). A comprehensive
 249 review of these methods can be found in Papan and Kugiumtzis (2008). Although the
 250 histogram binning technique is one of the most commonly used techniques (for example
 251 Campuzano et al. (2018); Pothapakula et al. (2019); Shin et al. (2023)), it introduces
 252 uncertainty. There are several techniques to estimate this uncertainty, such as the one
 253 proposed in Knuth et al. (2005). In this article, we use histograms with equidistant
 254 partitioning where constant optimal bin widths are determined using the Freedman-
 255 Diaconis rule (Freedman & Diaconis, 1981; Knuth, 2019) at each grid point to get a

discrete probability distribution. The same bin width was used for the marginal and joint probability distributions. Two approaches were used to estimate the sensitivity of the metric to binning: varying the bin width around the optimal value and bootstrapping over the ensemble members. The metrics were found to be more sensitive to changes in the bin widths than to bootstrapping. Therefore, to estimate uncertainty, if the width of the bin was found to be δw , then it was varied from $0.5\delta w$ to $1.5\delta w$ to obtain a reasonable estimate of uncertainty. Sweeping across the number of bins was performed also in (Sane et al., 2021) to get an estimate of predictability time-scale.

2.1.2 Information theory based metric

Using f and g , we propose the following metric γ , which has the same intent as metrics in (Leroux et al., 2018) to quantify the fraction of variability that is intrinsic, i.e., the typical amount that is unique to an ensemble member or statistical instance, but unlike (Leroux et al., 2018) this metric is built from standard information theory quantities:

$$\gamma = 1 - \frac{I(f;g)}{H(f)}. \quad (7)$$

$H(f)$ is the Shannon entropy of f , and $I(f;g)$ is mutual information between f and g . $I(f;g)$ calculates the contribution of extrinsic signal g to the whole ensemble. $H(f)$ is the total variability in the ensemble output which is the result of extrinsic and intrinsic factors. The metric γ gives *ratio of intrinsic variability to total variability*. When $f \rightarrow g$, then $I(f;g) \rightarrow H(f) = H(g)$ from (2). This makes $\gamma = 0$ when there is no intrinsic variability or chaos. When intrinsic chaos fully dominates the ensemble output, i.e. f and g are fully decorrelated, then $I(f;g) = 0$ yielding $\gamma = 1$. We see that γ satisfies the extremes of zero noise and total chaos.

Related quantities appear in other applications. The quantity $I(f;g)/H(f)$ is defined as ‘‘uncertainty coefficient’’ (Eshima, 2020). It is the ratio of entropy of f explained by g . $H(f)$ and $I(f;g)$ are related through conditional entropy by $H(f) = I(f;g) + H(f|g)$ (Cover, 1999). $H(f|g)$ is the conditional entropy $H(X|Y) = \sum p(x|y) \log_2 p(x|y)$ (Cover, 1999). It is not necessary to calculate the conditional entropy to arrive at γ . $H(X|Y)$ gives the average uncertainty about the value of f after g is known, or just the uncertainty in f that is not attributed to g but is attributed to η . Hence $H(f) - I(f;g)$ estimates variability due to intrinsic chaos and γ gives the fraction of the variability due to intrinsic chaos.

$I(f;g)$ takes into account any correlation or information shared between f and g . This is vital because even though the spread of the model η is treated similarly to the noise added to the mean signal, it might be that the spread of the model depends on the mean signal. A simple example is that if the model spread is relative (e.g., 10% of the mean signal, or *multiplicative noise*), rather than absolute (e.g., 2 units, or *additive noise*), then there is information about the model spread contained in the ensemble mean signal. The nonlinear and chaotic nature of fluids often leads the mean flow to amplify the chaotic signal (e.g., eddies) and thereby result in altered variability statistics that can be represented as multiplicative noise.

Returning to the binary tree analogy, $I(f;g)$ would be the set of instructions sent by a source to reach one among $2^{H(f)}$ possible destinations in the presence of noise having $H(f|g)$ entropy. To capture the entropy in the noisy binary tree, to each of the $2^{I(f;g)}$ micro-state possibilities, noise ($2^{H(f|g)}$) gets multiplied and the relation becomes $2^{H(f)} = 2^{I(f;g)} 2^{H(f|g)}$. Another analog of a component of the climate system is a noisy communication channel as given in Leung and North (1990), where the governing equations of ocean (atmosphere) modeling are taken to communicate from forcing to response. The extrinsic forcings are inputs to the channel, the intrinsic chaos is the noise created because of channel’s inherent mechanisms, while the outputs are

300 the ensemble members. A noiseless channel will give γ as zero, and a completely noisy
 301 channel where the output is independent of the input will give γ as 1.

302 A seemingly enticing and simpler alternative is $\gamma = 1 - \frac{H(g)}{H(f)}$, i.e. just the
 303 difference between the entropy of the ensemble and the mean entropy as a ratio with
 304 the entropy of the ensemble. However, this formulation is incorrect because $H(g)$ does
 305 not quantify the contribution of extrinsic factors to the variability in the ensemble, it
 306 only quantifies the variability of the mean. Relatedly, $H(f) - H(g)$ does not correctly
 307 manage the mutual information between the ensemble members and their mean in
 308 estimating intrinsic variability.

309 Another alternative was proposed by (Gomez, 2020): using Shannon entropy
 310 directly as a measure of intrinsic variability. They propose using Shannon entropy of
 311 model spread $\eta(n, t)$ at each time step normalized by the logarithm of the number of
 312 bins utilized. Their metric has a lower limit of 0 and an upper limit of 1, where 0
 313 denotes zero noise and hence zero intrinsic variability and 1 denotes complete intrinsic
 314 variability. Again, this metric is similar to γ in building upon information theory, but
 315 γ takes into account the variability of the ensemble mean, the correlations between
 316 the ensemble mean and the intrinsic variability, and it is time invariant. A time-
 317 dependent version of γ can be made using running time windows instead of the whole
 318 time series, but care in quantifying or controlling for lack of stationarity is needed
 319 in this interpretation (DelSole & Tippett, 2018). The Gomez (2020) metric uses the
 320 spread of the ensemble members similar to measuring Shannon entropy, whereas γ
 321 utilizes, in an abstract sense, the set of instructions required to choose a destination
 322 for the particular variable among the possible model states.

323 **2.1.3 Variance based metric**

A variance based metric as given in (Leroux et al., 2018) has been utilized to com-
 324 pare with our information-based metric. The variance-based metric measures intrinsic
 and extrinsic variability using the second moment, variance. It involves calculation of
 the following terms σ_g and σ_η given by:

$$\sigma_g^2 = \frac{1}{M} \sum_{t=1}^{t=M} \left(g(t) - \overline{g(t)} \right)^2, \quad (8)$$

$$\sigma_\eta^2(t) = \frac{1}{N} \sum_{n=1}^N \eta(n, t)^2, \quad (9)$$

where the overbar denotes the temporal averaging. Total variability has been estimated
 as $\left(\sigma_g^2 + \overline{\sigma_\eta^2(t)} \right)^{1/2}$. The forced variability σ_g is equivalent to $I(f; g)$, and the total
 variability $\left(\sigma_g^2 + \overline{\sigma_\eta^2(t)} \right)^{1/2}$ is equivalent to $H(f)$. Therefore, γ is compared to γ_{std}
 given by

$$\gamma_{std} = \frac{\left(\overline{\sigma_\eta^2(t)} \right)^{1/2}}{\left(\sigma_g^2 + \overline{\sigma_\eta^2(t)} \right)^{1/2}} \quad (10)$$

324

325 **2.2 Part B: Information Entropy and Boundary Forcing**

326 **2.2.1 Impact of changes in boundary forcings in coastal models**

327 Here instead of using the new metric γ , we use its components– Shannon entropy
 328 and mutual information–individually to compare variability between different simula-
 329 tions. Quantifying differences because of modifications in the extrinsic forcings may

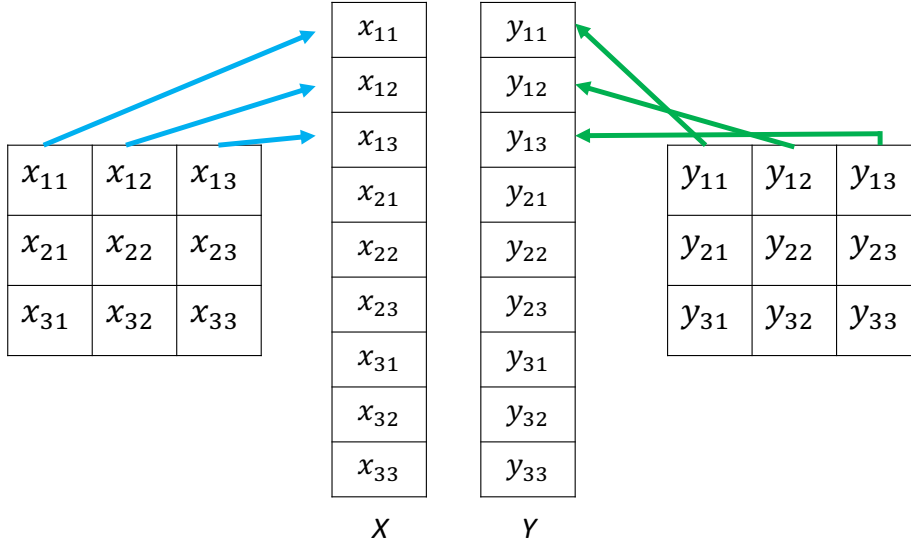


Figure 2. Flattening process for comparing two-dimensional fields using Shannon entropy and mutual information. As the flattened arrays x_1, x_2, \dots and y_1, y_2, \dots may not have linear dependence on each other, using linear dependence measures such as Pearson’s correlation might produce incorrect results. Mutual information measures nonlinear correlations and hence captures all linear and nonlinear dependence.

330 be required for coastal applications where systems vary predominantly due to external
 331 forcings. For these forcing significance experiments, OSOM was run after modifying
 332 the external forcings (Table 1). OSOM is forced by tides, river runoff, atmospheric
 333 winds, air-sea fluxes, etc. All model details can be found in Sane et al. (2021). For
 334 this comparison, we quantify the effects of altering forcing on 4 modeled variables: sea
 335 surface temperature and salinity, and bottom temperature and salinity. One control
 336 and four altered forcing sets were utilized,

- 337 1. (Control) Full atmospheric forcing using the North American Mesoscale (NAM)
 338 analyses, a data-assimilating, high resolution (12 km) meteorological simulation
 339 ([https://www.ncei.noaa.gov/data/north-american-mesoscale-model/access/
 340 historical/analysis](https://www.ncei.noaa.gov/data/north-american-mesoscale-model/access/historical/analysis)) denoted FF. FF stands for full forcing.
- 341 2. Full set of atmospheric forcing, but using the winds of the Northeast Coastal
 342 Ocean Forecast System (NECOFS) winds (Beardsley & Chen, 2014) instead of
 343 NAM, denoted as NECOFS.
- 344 3. River flows are replaced with their monthly averaged flow, other forcing as in
 345 FF
- 346 4. River flows set to zero, other forcing as in FF.
- 347 5. Wind forcing set to zero, other forcing as in FF.

348 These forcing sets have been tabulated in Table 1. The aim is to quantify the effect on
 349 total variability by removing or altering one of many processes that might contribute.

350 To evaluate spatial Shannon entropy, the spatial output at a particular instant in
 351 time was rearranged into a row vector by a process called flattening, as shown in Fig-
 352 ure 2. Land mask points were removed. A variable x , which is a two-dimensional vari-
 353 able, was converted to one-dimensional array (flattened) by concatenation. Shannon

Forcing Set	Wind forcing	River forcing
FF	NAM	As Observed
NECOFS	NECOFS	As Observed
MR	NAM	Time-averaged rivers
ZR	NAM	Zero river input
ZW	Zero winds	As Observed

Table 1. Different types of forcing combinations were used to test their effect on variability. FF stands for full forcing: winds, tides, rivers, etc. For more details, see Sane et al. (2021). MR: mean rivers; ZR: zero rivers; ZW: zero wind.

354 entropy was found for the flattened variable at each time step to obtain a time-varying
 355 entropy of each surface or bottom variable.

356 Mutual information was applied between the flattened row vectors. Our focus is
 357 on a pragmatic approach to using information theory for relative comparisons among
 358 simulations, rather than an equation for the evolution of Shannon entropy and mutual
 359 information with respect to time (see X. S. Liang and Kleeman (2005)). For example,
 360 if mutual information on surface salinity between FF and MR is higher than between
 361 FF and ZR, this implies that the penalty for using time-averaged river runoff is not
 362 as severe as using zero river runoff. The replacement of FF with MR will give more
 363 similar results to FF than replacing FF with ZR will. We can interpret this to indicate
 364 that small errors in river runoff flow rates will not cause appreciable changes to surface
 365 salinity while using zero rivers will strongly impact the solution.

366 3 Results

367 3.1 Part A: Intrinsic and Extrinsic Variability Results for Ensemble Data

368 3.1.1 Idealized Gaussian Arrays

369 We test our metric γ , equation (7) on synthetic data consisting of idealized arrays
 370 of Gaussian data: $\mathcal{N}(0, 1)$. For a normal Gaussian distribution Shannon entropy
 371 depends¹ only on the standard deviation σ . The variability in a Gaussian distribution
 372 can be increased or decreased by changing its standard deviation. Our goal is to
 373 compare γ and γ_{std} . We set out our numerical experiment as follows: we create 10
 374 arrays, each having 10,000 elements drawn from a Gaussian distribution. Any two
 375 arrays from those 10 have a prescribed correlation coefficient between 0 and 1.

376 Thus, the 10 arrays are linearly correlated with a specified correlation coefficient.
 377 These 10 arrays represent ensemble members from climate simulations. The mean of 10
 378 members gives us the synthetic forced variability signal as would be determined from
 379 the model output; averaging over the 10 ensemble members reduces the contribution
 380 from uncorrelated variability and reaffirms the covarying component into the forced
 381 variability. We apply γ and γ_{std} on this synthetic ensemble by varying the prescribed
 382 correlation coefficient from 0 to 1. Figure 3 shows that, as expected, both metrics
 383 increase as the correlation decreases, that is, as internal variability dominates forced.

¹ $H = -\log_2 2\pi e\sigma^2$ is the Shannon entropy of a Gaussian distribution when probability density is continuous with σ as standard deviation. The Shannon entropy of a discrete probability distribution differs, which is inconsequential here, but the reader is encouraged to read Jaynes (1962). Throughout this article, discretely sampled and binned probability distributions are obtained directly from the data without any further parameterization

Both metrics behave similarly when correlation decreases, i.e., noise increases, but γ is more sensitive as correlation tends to 1. This distinction is due to the logarithmic nature of Shannon entropy for Gaussian distributions—in essence, information measured in bits is not proportional to distance measured between distributions in terms of summed variance—in the examples following the consequences of this distinction will become clearer. Critically, both functions are monotonic with correlation; however, relative comparisons (more intrinsic fraction in one region vs. a different region) are preserved.

A second related experiment was derived from the first and is also shown in Figure 3: adding outliers outside of the Gaussian distribution. 50 out of 10000 elements of each individual member were artificially corrupted (values were set to a constant value of 5) to test the sensitivity of both metrics. Figure 3 shows that γ is insensitive to outliers while γ_{std} is not. γ is not sensitive because outliers occur less frequently and therefore do not greatly affect the probability distribution, especially with the prefactor in (1) and (2). Hence, information theory metrics are robust in comparison to using standard deviation (or variance). If the outliers (extreme events) occur at higher frequencies, information metrics will naturally start sensing them even if they are discontinuous from the typical conditions (e.g., multimodal distributions). The above process was repeated for 100 ensemble members, each sampled from Gaussian distributions. Increasing the number of ensemble members does not change the result qualitatively for both experiments. The results for a Gaussian ensemble of 10 members are shown in Figure 3 a and 100 members in Figure 3 b.

Additionally, a set of experiments was carried out using uniformly distributed data $U(-1, 1)$. The prescribed correlated vectors were created using the procedure described in Demirtas (2014). 10 and 100 ensemble members were created and γ and γ_{std} were found between the members and their mean. The results are shown in Figure 3 c, d, respectively. The outlier had a value of 1.5. In all cases, γ was less sensitive to outliers than γ_{std} .

3.1.2 Regional coastal model output

In this section we show the results of applying γ and γ_{std} on realistic simulation data from the Ocean State Ocean Model, hereafter OSOM (Sane et al., 2021). OSOM uses the Regional Ocean Modeling System (ROMS) (Shchepetkin & McWilliams, 2005) to model Narragansett Bay and the surrounding coastal oceanic regions and waterways. OSOM’s primary purpose is to understand and predictive modeling and forecasting of the estuarine state and climate of this Rhode Island body. Sane et al. (2021) gives more details about the model.

Using OSOM, an ensemble of simulations has been performed using perturbed initial (ocean) conditions under the same atmospheric and tidal forcing for the months July and August of 2006. This ensemble consists of 10 members. Data during the first predictability window (20 days) where results are still linked directly to the initial conditions have been ignored and the remaining simulation has been used to examine variability within the “climate projection” of the model beyond when forecasts or predictions that rely deterministically on initial conditions are possible. During this phase the different ensemble members visit different possible futures within the envelope of the projected “climate” (see the related application of information theory to assess predictability in Sane et al. (2021)). The modeled temperature and salinity at each grid point typically do not follow Gaussian distributions as the skewness and kurtosis each grid point shown in Figure 4 for salinity and temperature of the sea surface and bottom for the Narragansett Bay region. The horizontal axis shows skewness and excess kurtosis, which are the third and fourth statistical moments, respectively, normalized by powers of the standard deviation to dimensionless ratio, and in the

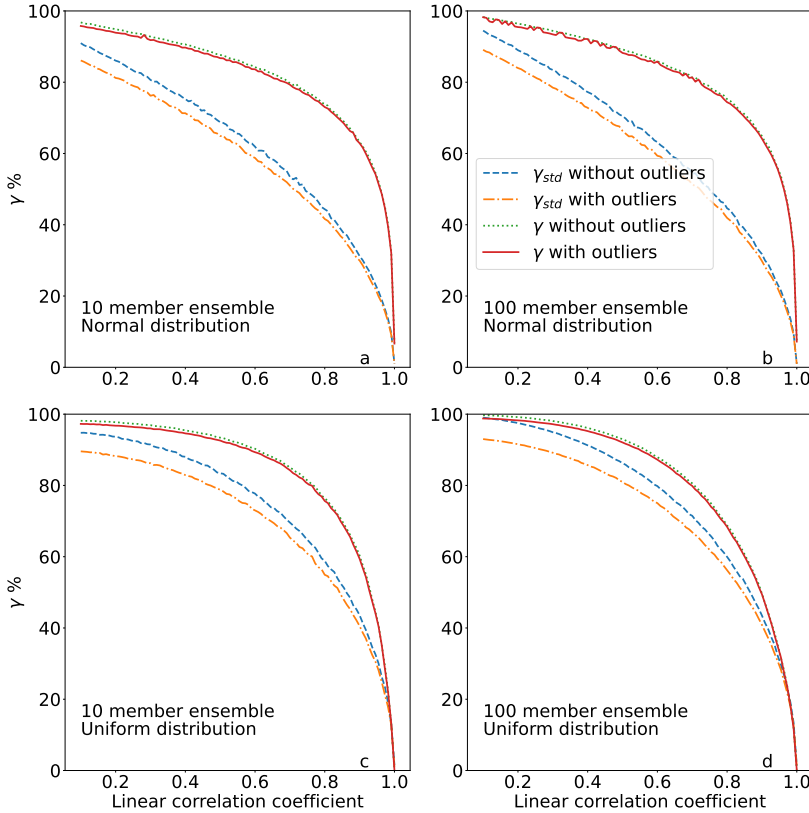


Figure 3. Information theory metric of intrinsic vs. extrinsic variability γ as a function of the correlation coefficient in idealized Gaussian correlated arrays (a and b) and idealized uniformly distributed arrays (c and d). The horizontal axis is the correlation coefficient between the mean member and ensemble members. The vertical axis shows the information theory metric γ from (7) and the traditional metric γ_{std} from Equation (10). A second related experiment is also shown adding (50 out of 10,000) “corrupted” outliers to each individual member. The information theory metric γ does not change for these outliers, which shows its robustness, while γ_{std} is highly sensitive. The results are similar for Gaussian distribution members and uniformly distributed members. γ is more sensitive around linear correlation of 1. This is due to the logarithmic nature of γ .

435 case of excess kurtosis a constant value of 3 is subtracted. For Gaussian distributions,
 436 both skewness and excess kurtosis should be close to zero. The vertical axis denotes
 437 the number of occurrences at a grid point. Observe that the majority of grid point
 438 values are away from zero and thus these variables are considerably non-Gaussian in
 439 OSOM. Therefore, the variance method in Equation (10) is at a disadvantage because
 440 the prevalence of higher statistical moments implies that the variance does not contain
 441 a complete description of the variability. The information theory metric (7) is suitable
 442 for such data as it takes into account higher moments and does not rely on Gaussian
 443 distributions.

444 Figure 7 shows the ratio of intrinsic variability to total variability applied at every
 445 point in the OSOM grid. γ_{std} is displayed on left whereas γ is shown in the center for
 446 comparison. The uncertainty in γ has been plotted in the third column in Figure 7.
 447 The features highlighted by both metrics are qualitatively different. The contribution

448 of intrinsic chaos to total variability is more uniform using the γ metric than using γ_{std} .
 449 The intrinsic chaos displayed using γ_{std} might be misleading because the probability
 450 distributions are non-Gaussian. Furthermore, where the γ metric highlights internal
 451 variability, it tends to agree in similar dynamical locations—all river mouths show high
 452 surface salinity intrinsic variability. While surface temperature intrinsic variability
 453 is higher in more open regions of the Bay, where eddies form intermittently due to
 454 varying topography. Also note that the ranges are quite different between γ and γ_{std} ,
 455 but this is to be expected from the different rate of increase with correlation seen in
 456 Figure 3. The Eastern North-South passageway of the bay shows different structure
 457 of γ than γ_{std} of salinity.

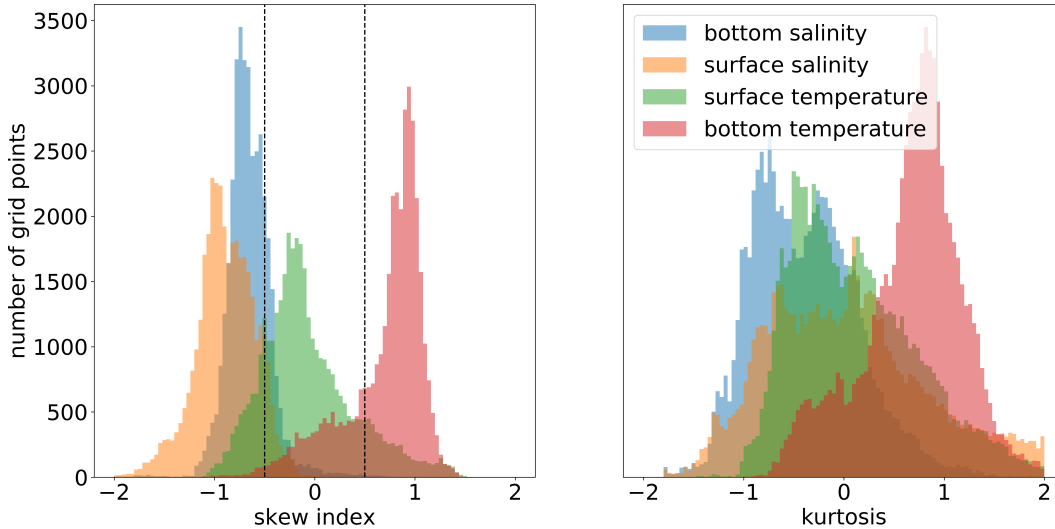


Figure 4. Grid point-wise skewness and excess kurtosis for OSOM output. Neither are close to zero, e.g., within $(-0.5, 0.5)$, suggesting that the temperature and salinity data distribution is non-Gaussian.

3.1.3 Earth System Model Large Ensemble

458

459 A complementary experiment was performed using γ to evaluate internal versus
 460 forced variability in global climate simulation output for the RCP8.5 climate change
 461 scenario using the GFDL-LE model (randomly selected among the models compared).
 462 The 30 members of the ensemble were utilized. The variability of sea surface temper-
 463 ature (Figures 5) and sea surface salinity (Figures 6) were estimated using both γ and
 464 γ_{std} .

465 Note in particular the Arctic sea surface temperatures in Figure 5, which have a
 466 highly skewed and excessive kurtosis distribution due to the freezing point of seawater.
 467 The standard metric (γ_{std}) considers this region to be among the most intrinsically
 468 variable in the world, while the information theory metric considers it as a region of
 469 middling intrinsic variability—much lower than the equatorial regions where El Nino
 470 variability is profound. This region is also subject to intermittent and drastic swings
 471 in salinity as sea ice forms and melts, but note that the standard metric indicates low
 472 salinity variability while the information theory metric ranks it as high in Figure 6. It
 473 is clear that a Gaussian metric should not be applied to the Arctic due to the skewness
 474 and excess kurtosis, and in this case the inference is opposite using the standard and
 475 information theory metrics. In the equatorial Pacific, where Gaussian statistics are
 476 more reliable, the two metrics agree that internal variability is high.

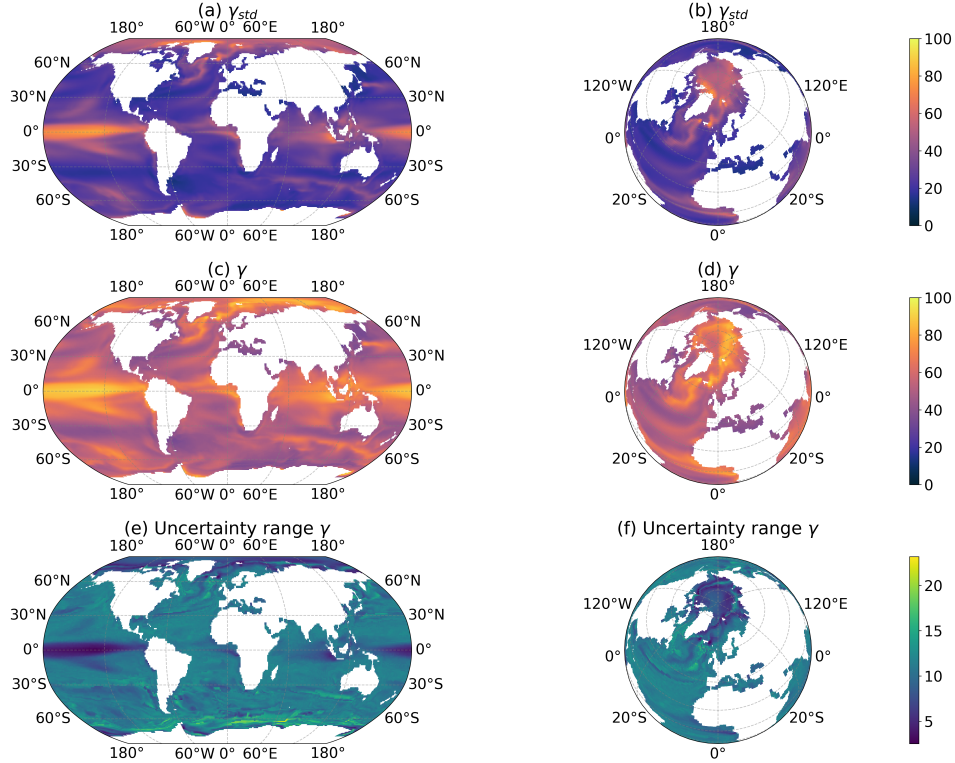


Figure 5. Intrinsic to total variability for sea surface temperature using (a, b) γ_{std} and (c, d) γ . (e, f) Uncertainty range in γ found by sweeping across the bin width as explained in the text. We can see a difference in the magnitude and pattern of the intrinsic to total variability around the Arctic region. Difference in other regions such as Mediterranean sea and Pacific equator is also visible.

477 A less drastic failure occurs from the modest excess kurtosis in extratropical
 478 temperatures and in a few isolated regions in surface salinity. These regions are also
 479 non-Gaussian but are also not heavily skewed (i.e., they are more long-tailed and
 480 intermittent than Gaussian). These regions differ in the relative estimation of intrinsic
 481 versus total variability. It is also the case that the γ metric is closer to one in
 482 most regions than γ_{std} , which is expected when the correlation coefficients are low in
 483 Figure 3.

484 3.2 Part B: Information Entropy and Boundary Forcing Results

485 3.2.1 Impact due to changes in boundary conditions in coastal models:

486 We show the results of the coastal model analysis under different forcing in
 487 Figures 8 and 9, under the same region as shown in Figure 7. The entropy has been
 488 plotted with respect to time as some variability occurs. In Figure 8, Shannon entropy
 489 is plotted for spatial quantities. For example, for surface salinity, all surface values
 490 have been considered to find the Shannon entropy using the flattening approach. If
 491 Shannon entropy is more or less equal for two forcings, it implies that they similarly
 492 affect variability. Both winds and rivers seem to have similar effects in this regard.
 493 However, Figure 9 displays mutual information which should be compared for two
 494 pairs of forcings. Greater mutual information implies that the two pairs share more

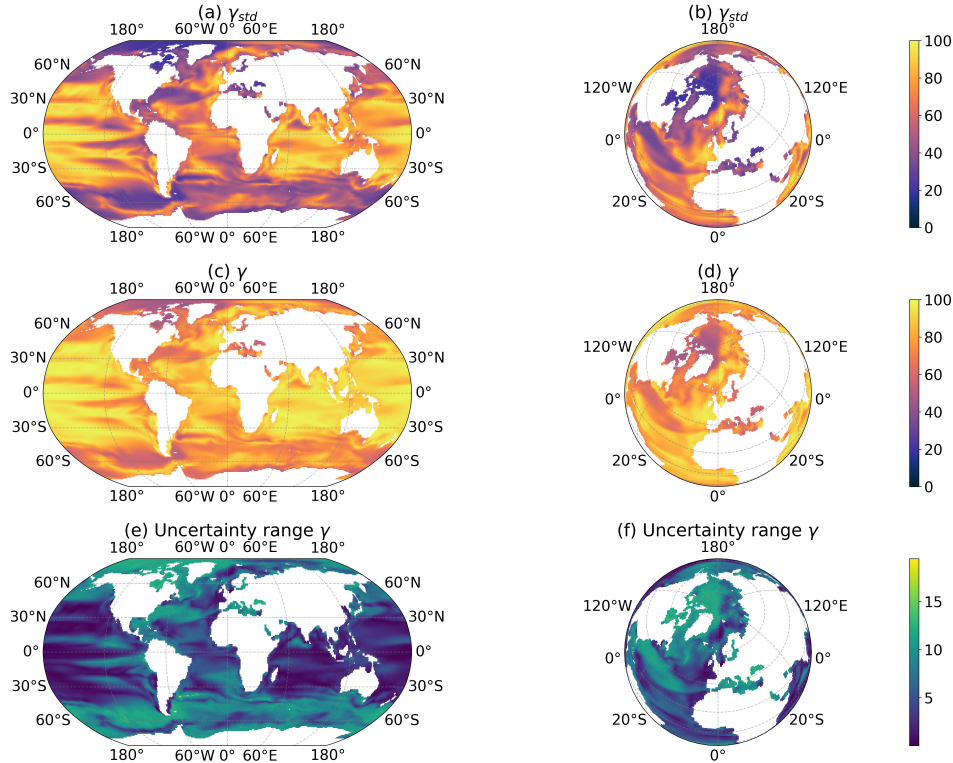


Figure 6. Intrinsic to total variability for sea surface salinity using (a, b) γ_{std} and (c, d) γ . (e, f) Uncertainty range in γ by sweeping across the bin width as explained in the text. We can see a difference in the magnitude and pattern of the intrinsic to total variability around the Arctic region. Difference in other regions such as Mediterranean sea and Pacific equator is also visible

495 *bits* of information, suggesting that one of the forcing in that pair can be replaced
 496 with the other without significantly affecting variability. For temperature dependence
 497 on wind in Figure 8, we see that only NAM and NECOFS, our two realistic forcing
 498 conditions, share much mutual information. Figure 9 shows zeroing the rivers strongly
 499 reduces the salinity variability. Furthermore, in terms of salinity impact, full rivers and
 500 mean rivers share information as do NAM and NECOFS wind forcing.

501 4 Discussion

502 Our numerical experiments performed using γ on idealized Gaussian arrays show
 503 that γ is monotonic and decreases as the linear correlation coefficient increases. Thus,
 504 apart from the qualitative differences the new metric finds when the data are non-
 505 Gaussian, the ranges of intrinsic versus total variability are quite different between γ
 506 and γ_{std} . This is to be expected from the different rates of increase with correlation
 507 seen in Figure 3. The traditional metric (γ_{std}) falls approximately linearly as the
 508 correlation coefficient increases, so that a correlation coefficient of 0.5 gives a γ_{std} just
 509 above 0.5. The new metric γ agrees with γ_{std} that a correlation of 0 implies $\gamma = 1$, and
 510 a correlation of 1 implies $\gamma = 0$, but for a correlation of 0.5 it is closer to $\gamma = 0.9$. Only
 511 very near the correlation coefficients of 1 does γ fall below 0.5. If a roughly linear
 512 dependence on the correlation coefficient is desired, γ can be raised to a power— γ^3
 513 resembles γ_{std} and γ^6 resembles the correlation coefficient. These higher powers do
 514 not lose the ability to apply to non-Gaussian data nor become non-monotonic, but

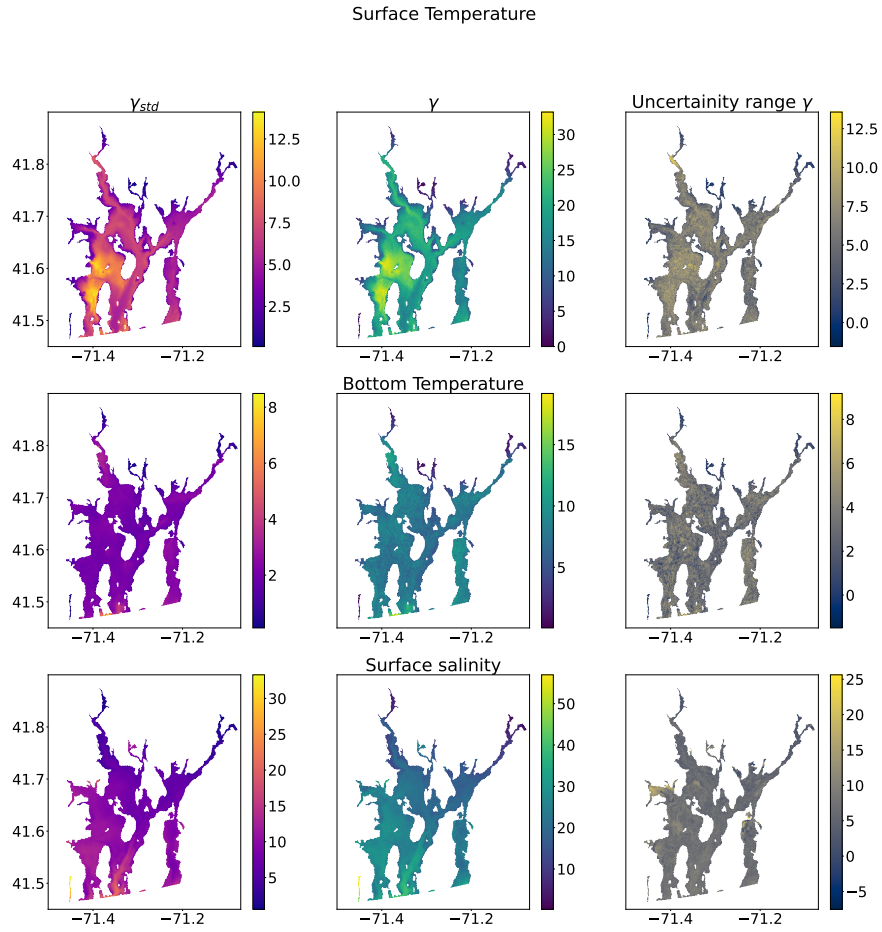


Figure 7. Metrics γ vs γ_{std} for the OSOM output. Both metrics show different contributions of intrinsic variability to total variability. γ is more uniform in the domain than γ_{std} . Right panels show the uncertainty in γ due to binning choices. The color maps for γ and γ_{std} are different to highlight their different ranges. γ_{std} for bottom temperature (not shown) has a maximum value of 5%, and the pattern is almost uniform except at the river sources where the values are on the lower side (less than 1%).

Surface Temperature

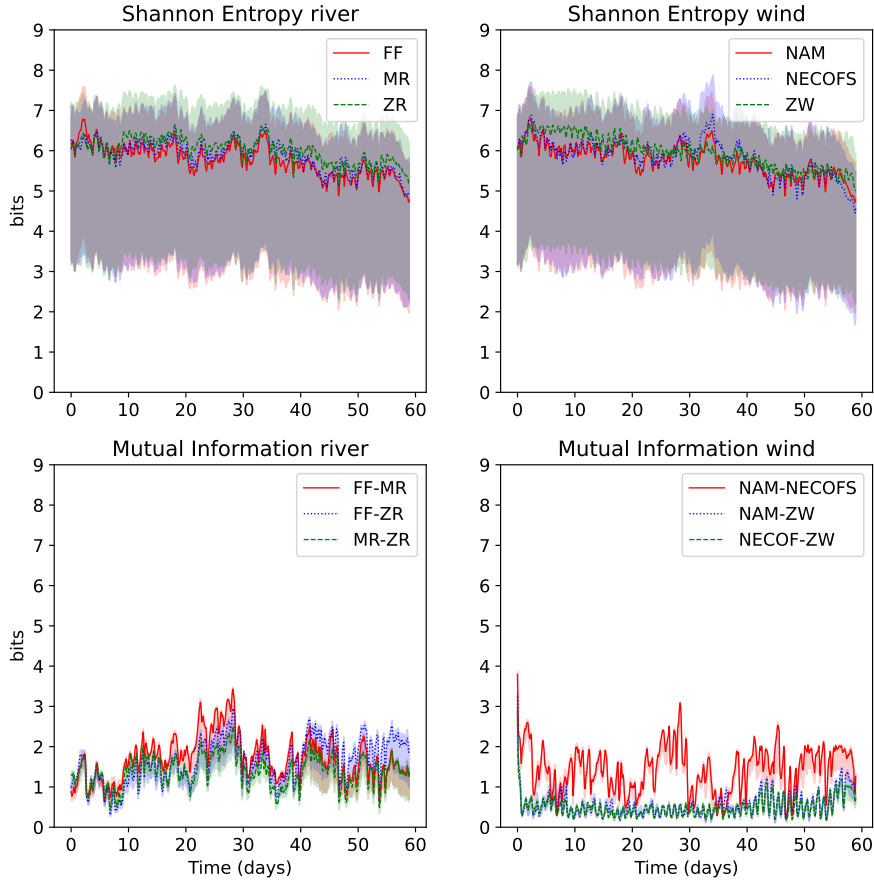


Figure 8. Shannon entropy applied to temperature and salinity. Replacing fully time-varying rivers with monthly mean river flow gives almost the same result for salinity. The same is true by replacing the wind product with a different one. Setting the river to zero affects salinity, but not temperature. Winds are important in terms of variability, but different wind products do not noticeably alter variability.

515 they will lose their interpretation as a ratio of bits of information entropy, and instead
 516 reflect ratios of bits cubed of information entropy, etc. An alternative is to take γ_{std}
 517 raised to a different power: $\gamma_{std}^{1/3}$ is roughly similar to γ .

518 The uncertainty associated with binning is small—typically much less than the
 519 variability across the domain and the metrics are thus not overly sensitive to the
 520 binning procedure. The exploration of alternative strategies to evaluate entropies will
 521 remain a topic of future investigation and may further improve precision.

522 As can be seen in Figures 7, 5, and 6, information theory metrics show differ-
 523 ent patterns compared to variance metrics. Information theory metrics, especially
 524 mutual information, account for *all* non-linear shared information between the en-
 525 semble members and the mean including linear correlation, and this is one reason for

Surface Salinity

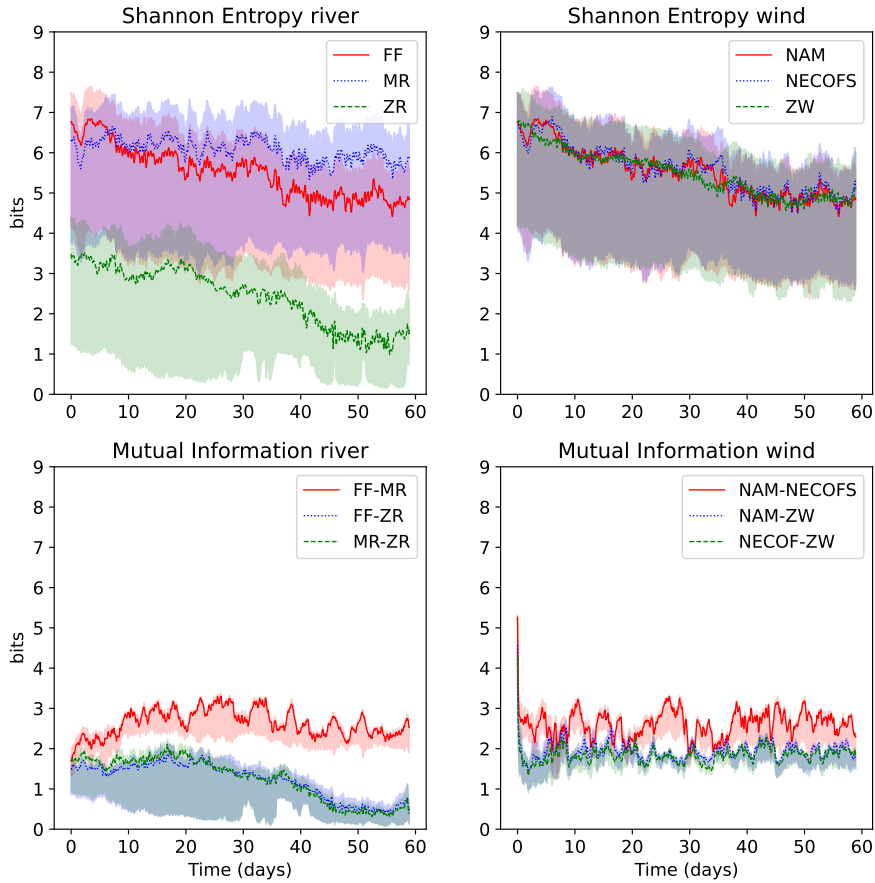


Figure 9. Mutual information applied to simulations from different forcings. Higher mutual information implies higher similarity in terms of variability. For example, NAM-NECOFS values are higher than NAM-ZW implying that NAM and NECOFS are significantly different than having no wind.

526 the differences. We have argued that non-Gaussian statistics are another (which is
 527 not wholly independent of non-linear shared relationships). There are likely other aspects
 528 of differences between these metrics, but the management of these two expected
 529 aspects of geophysical fluids—nonlinear relationships and non-Gaussian distributions—
 530 —justifies analyzing the data with nonparametric metrics in addition to second moment
 531 statistics.

532 For the regional coastal model OSOM, forcings differ in shared information and
 533 as to how they affect different variables. As might be expected, river runoff is more
 534 important for salinity than for temperature. However, for July to August, replacing
 535 rivers with the monthly mean river flow gives nearly the same result (in terms of variability)
 536 as fully time-varying rivers. Similarly, averaging the river runoff gives a similar
 537 effect for salinity compared to giving the observed river runoff in the simulations; see
 538 Figure 8. This might be due to lower river runoff during summer leading to lower

539 variability in the flow rate hence averaging river runoff might be appropriate. We can-
 540 not conclude if there will be a similar effect in winter because the higher river runoff
 541 lead to larger variability and replacing river runoff with its mean might be unfruitful.
 542 Temperature is less sensitive to any of the forcing alterations, because it has different
 543 sources and sinks than salinity. Switching the wind product from NAM to NECOFS
 544 does not have a significant effect on the sources or sinks of temperature or salinity,
 545 but switching the wind off definitely affects the parameters by eliminating wind-driven
 546 mixing altogether. Figure 9 shows that zero-wind (ZW) simulations are markedly dif-
 547 ferent from the rest in terms of *mutual information* (i.e. they do not covary), although
 548 very similar in terms of amount of spatial variability (Shannon entropy, Figure 8), be-
 549 cause even without winds tides, fluxes, and rivers still vary. The zero-river case tends
 550 to eliminate both variability and mutual information (ZR).

551 If we were to prioritize improvements based on Shannon entropy and mutual
 552 information, note that the two highest mutual information cases are where NAM is
 553 substituted with NECOFS and where mean rivers are substituted for varying rivers.
 554 The first observation is important from a forecast perspective, because it means that we
 555 cannot easily tell the difference between different wind products, although something
 556 rather than zero winds should be used if the estuary needs to be forecast for the
 557 full 20 day predictability range (weather forecasts are reliable for only about 7 days
 558 in this region). Similarly, knowing that substituting the mean of the rivers for fully
 559 varying rivers has little impact implies that rivers can be fixed in time for forecasts
 560 beyond where they might be predicted based on expected weather and precipitation.
 561 Finally, despite the fact that Narragansett Bay is a dominantly tidally mixed estuary,
 562 among the sources of overall variability (i.e. sources of information entropy) considered,
 563 preserving an inflow of fresh water is key, even though that inflow can be steady. Winds
 564 do not appreciably increase information entropy of the Bay, but they are an important
 565 source of forced co-variation, and so are important for predictions but do not raise the
 566 overall level of variability.

567 It should be noted that a major difference between coastal and global ensemble
 568 is in the way they are forced. The ocean in the coastal model has been forced by
 569 fixed atmosphere, tides, and rivers whereas the GFDL ESM2E has atmosphere which
 570 responds to the changes in the ocean. The intrinsic variability seen in the coastal
 571 ensemble is due to the ocean alone. The intrinsic variability observed in the global
 572 ensemble might not just be due to the ocean alone but might have all the possible
 573 sources present in the coupled system.

574 5 Conclusion

575 We showed usage of information theory metrics to determine contribution of in-
 576 trinsic chaos and external variability to total variability in ensemble model simulations.
 577 The metric consists of Shannon entropy and mutual information and is non-parametric
 578 compared to variance. We have applied metrics on idealized Gaussian arrays, as well
 579 as realistic coastal ocean and global climate models. We conclude that:

- 580 1. The information theory metric is more reliable when outliers are present, because
 581 outliers get assigned less probability and because Gaussian distributions have a
 582 difficult time approximating long-tailed (i.e., outlier-prone) distributions.
- 583 2. The information theory metric is more reliable when variability is non-Gaussian
 584 because it is based on nonparametric measures of the probability distributions
 585 and captures nonlinear correlations.
- 586 3. The new information theory metric varies monotonically with ensemble member
 587 to ensemble mean correlation, but is quantified in fractions of bits required to
 588 capture internal variability versus bits required to capture total variability.
 589

- 589 4. The use of the information theory ratio metric in a coastal ocean model ensemble
 590 and a climate model ensemble qualitatively changes the focus to regions that
 591 were previously erroneously labeled as having high or low internal variability.
- 592 5. The use of Shannon entropy and mutual information can quickly focus atten-
 593 tion on which forcing choices cause the most variability and need attention as
 594 their substitutions significantly affect the outcomes. These conclusions can be
 595 drawn regardless of the fact that the dimensions of wind, rivers, salinity, and
 596 temperature have no specified unit conversion factors.
- 597 6. In these ensemble simulations, the coastal ensemble had a much smaller intrinsic
 598 (chaotic) proportion of its total variability in comparison to the climate ensemble
 599 which had more intrinsic variability (weather, climate oscillations, etc.) as a
 600 proportion of its total. Importantly, the resolution of the models helps determine
 601 the proportion of intrinsic variability, so such comparisons are model-specific: a
 602 higher-resolution coastal model might well have a larger intrinsic fraction than
 603 a coarser climate model.
- 604 7. For the global simulations, Arctic ocean is known to be salinity dominated and
 605 temperature plays the role of a passive tracer when near the freezing point
 606 (Timmermans & Jayne, 2016), (MacKinnon et al., 2016) Information theory
 607 metric γ clearly shows high intrinsic variability in temperature at the Arctic
 608 and extrinsic forcing is low to moderate. This implies the intrinsic variability in
 609 temperature is extraneous to the dynamics of the Arctic Ocean.

610 Other applications of these and similar information theory metrics are likely to
 611 be revealing of new behavior and sensitivity of models.

612 **6 Data Availability Statement**

613 We have made the code and data available at [https://doi.org/10.5281/zenodo](https://doi.org/10.5281/zenodo.7992844)
 614 [.7992844](https://doi.org/10.5281/zenodo.7992844). The GFDL-ESM2M Large Ensemble climate model data can be accessed
 615 from <https://www.cesm.ucar.edu/community-projects/mmlea> and has been de-
 616 scribed in (Rodgers et al., 2015) and (Deser et al., 2020).

617 **Acknowledgments**

618 The Rhode Island Coastal Ecology Assessment Innovation & Modeling grant
 619 (NSF 1655221) supported this work. B. Fox-Kemper was also supported by ONR
 620 N00014-17-1-2963. This material is based upon work conducted at a Rhode Island
 621 NSF EPSCoR research facility Center for Computation and Visualization (Brown Uni-
 622 versity), supported in part by the National Science Foundation EPSCoR Cooperative
 623 Agreement OIA 1655221.

624 **References**

- 625 Beardsley, R. C., & Chen, C. (2014). Northeast coastal ocean forecast system
 626 (necofs): A multi-scale global-regional-estuarine fvcom model. *AGUFM, 2014*,
 627 OS23C-1211.
- 628 Brissaud, J. B. (2005). The meanings of entropy. *Entropy, 7*(1), 68–96. doi: 10
 629 .3390/e7010068
- 630 Campuzano, S., De Santis, A., Pavón-Carrasco, F. J., Osete, M. L., & Qamili, E.
 631 (2018). New perspectives in the study of the earth’s magnetic field and climate
 632 connection: The use of transfer entropy. *PloS One, 13*(11), e0207270.
- 633 Carcassi, G., Aidala, C. A., & Barbour, J. (2021). Variability as a better character-
 634 ization of shannon entropy. *European Journal of Physics, 42*(4), 045102.
- 635 Correa, C. D., & Lindstrom, P. (2013). The mutual information diagram for un-

- 636 certainty visualization. *International Journal for Uncertainty Quantification*,
637 3(3).
- 638 Cover, T. M. (1999). *Elements of information theory*. John Wiley & Sons.
- 639 DelSole, T., & Tippett, M. K. (2007). Predictability: Recent insights from informa-
640 tion theory. *Reviews of Geophysics*, 45(4).
- 641 DelSole, T., & Tippett, M. K. (2018). Predictability in a changing climate. *Climate*
642 *Dynamics*, 51(1), 531–545.
- 643 Demirtas, H. (2014). Generating bivariate uniform data with a full range of correla-
644 tions and connections to bivariate binary data. *Communications in Statistics-*
645 *Theory and Methods*, 43(17), 3574–3579.
- 646 Deser, C., Lehner, F., Rodgers, K., Ault, T., Delworth, T., DiNezio, P., . . . Ting, M.
647 (2020). Insights from earth system model initial-condition large ensembles and
648 future prospects [dataset]. *Nature Climate Change*, 1–10.
- 649 Eshima, N. (2020). Statistical data analysis and entropy. In (p. 13-14). Springer.
- 650 Frankcombe, L. M., England, M. H., Mann, M. E., & Steinman, B. A. (2015). Sep-
651 arating internal variability from the externally forced climate response. *Journal*
652 *of Climate*, 28(20), 8184–8202.
- 653 Franzke, C. L. E., Barbosa, S., Blender, R., Fredriksen, H.-B., Laepple, T., Lambert,
654 F., . . . Yuan, N. (2020). The structure of climate variability across scales.
655 *Reviews of Geophysics*, 58(2), e2019RG000657.
- 656 Freedman, D., & Diaconis, P. (1981). On the histogram as a density estimator:
657 L 2 theory. *Zeitschrift für Wahrscheinlichkeitstheorie und verwandte Gebiete*,
658 57(4), 453–476.
- 659 Gomez, B. G. (2020). *Intrinsic ocean variability modulated by the atmosphere in the*
660 *gulf of mexico: an ensemble modelling study* (Unpublished doctoral disserta-
661 tion). Université Grenoble Alpes [2020-....].
- 662 Hacine-Gharbi, A., Ravier, P., Harba, R., & Mohamadi, T. (2012). Low bias
663 histogram-based estimation of mutual information for feature selection. *Pat-*
664 *tern recognition letters*, 33(10), 1302–1308.
- 665 Hartley, R. V. L. (1928). Transmission Information. *Bell System Technical Journal*,
666 7(3), 535–563.
- 667 Hawkins, E., & Sutton, R. (2012). Time of emergence of climate signals. *Geophysical*
668 *Research Letters*, 39(1).
- 669 Jaynes, E. T. (1962). *Information theory and statistical mechanics* (Vol. 3). Brandies
670 University Summer Institute Lectures in Theoretical Physics.
- 671 Kleeman, R. (2002). Measuring dynamical prediction utility using relative entropy.
672 *Journal of the atmospheric sciences*, 59(13), 2057–2072.
- 673 Knuth, K. H. (2019). Optimal data-based binning for histograms and histogram-
674 based probability density models. *Digital Signal Processing*, 95, 102581.
- 675 Knuth, K. H., Golera, A., Curry, C. T., Huyser, K. A., Wheeler, K. R., & Rossow,
676 W. B. (2005). Revealing relationships among relevant climate variables with
677 information theory. In *Eart-sun system technology conference 2005*.
- 678 Kowal, R. R. (1971). 296. note: Disadvantages of the generalized variance as a mea-
679 sure of variability. *Biometrics*, 27(1), 213–216. Retrieved from [http://www](http://www.jstor.org/stable/2528939)
680 [.jstor.org/stable/2528939](http://www.jstor.org/stable/2528939)
- 681 Kowalski, A. M., Martin, M. T., Plastino, A., & Judge, G. (2012). On extracting
682 probability distribution information from time series. *Entropy*, 14(10), 1829–
683 1841. doi: 10.3390/e14101829
- 684 Leroux, S., Penduff, T., Bessières, L., Molines, J.-M., Brankart, J.-M., Sérazin, G.,
685 . . . Terray, L. (2018). Intrinsic and atmospherically forced variability of the
686 amoc: insights from a large-ensemble ocean hindcast. *Journal of Climate*,
687 31(3), 1183–1203.
- 688 Leung, L.-Y., & North, G. R. (1990). Information theory and climate prediction.
689 *Journal of Climate*, 3(1), 5–14.

- 690 Liang, X. S. (2013). The liang-kleeman information flow: Theory and applications.
691 *Entropy*, *15*(1), 327–360.
- 692 Liang, X. S. (2014). Entropy evolution and uncertainty estimation with dynamical
693 systems. *Entropy*, *16*(7), 3605–3634.
- 694 Liang, X. S., & Kleeman, R. (2005). Information transfer between dynamical system
695 components. *Physical review letters*, *95*(24), 244101.
- 696 Liang, Y.-C., Kwon, Y.-O., Frankignoul, C., Danabasoglu, G., Yeager, S., Cherchi,
697 A., . . . Tian, T. (2020). Quantification of the arctic sea ice-driven atmospheric
698 circulation variability in coordinated large ensemble simulations. *Geophysical*
699 *Research Letters*, *47*(1), e2019GL085397.
- 700 Llovel, W., Penduff, T., Meyssignac, B., Molines, J.-m., Terray, L., Bessières, L., &
701 Barnier, B. (2018). Contributions of atmospheric forcing and chaotic ocean
702 variability to regional sea level trends over 1993–2015. *Geophysical Research*
703 *Letters*, *45*(24), 13–405.
- 704 MacKinnon, J. A., Nash, J. D., Alford, M. H., Lucas, A. J., Mickett, J. B., Shroyer,
705 E. L., . . . Wagner, G. L. (2016). A tale of two spicy seas. *Oceanography*,
706 *29*(2), 50–61.
- 707 Majda, A. J., & Gershgorin, B. (2010). Quantifying uncertainty in climate change
708 science through empirical information theory. *Proceedings of the National*
709 *Academy of Sciences*, *107*(34), 14958–14963.
- 710 Milinski, S., Maher, N., & Olonscheck, D. (2019). How large does a large ensemble
711 need to be. *Earth Syst. Dynam. Discuss.*, *2019*, 1–19, doi: 10.5194/esd-2019,
712 *70*.
- 713 Johnson, L., Fox-Kemper, B., Li, Q., Pham, H., & Sarkar, S. (2023, May). A
714 finite-time ensemble method for mixed layer model comparison. *Journal of*
715 *Physical Oceanography*. Retrieved from [https://fox-kemper.com/pubs/
716 pdfs/JohnsonFox-Kemper23.pdf](https://fox-kemper.com/pubs/pdfs/JohnsonFox-Kemper23.pdf) (Accepted)
- 717 Papan, A., & Kugiumtzis, D. (2008). Evaluation of mutual information estimators
718 on nonlinear dynamic systems. *Nonlinear Phenomena in Complex Systems*,
719 *11*(2), 225–232.
- 720 Pothapakula, P. K., Primo, C., & Ahrens, B. (2019). Quantification of information
721 exchange in idealized and climate system applications. *Entropy*, *21*(11), 1094.
- 722 Rodgers, K. B., Lin, J., & Frölicher, T. L. (2015). Emergence of multiple
723 ocean ecosystem drivers in a large ensemble suite with an earth system
724 model [dataset]. *Biogeosciences*, *12*(11), 3301–3320. Retrieved from
725 <https://bg.copernicus.org/articles/12/3301/2015/> doi: 10.5194/
726 bg-12-3301-2015
- 727 Sane, A., Fox-Kemper, B., Ullman, D. S., Kincaid, C., & Rothstein, L. (2021).
728 Consistent predictability of the ocean state ocean model (osom) using in-
729 formation theory and flushing timescales. *Journal of Geophysical Research:*
730 *Oceans*, e2020JC016875. Retrieved from [https://agupubs.onlinelibrary
731 .wiley.com/doi/abs/10.1029/2020JC016875](https://agupubs.onlinelibrary.wiley.com/doi/abs/10.1029/2020JC016875) doi: [https://doi.org/10.1029/
732 2020JC016875](https://doi.org/10.1029/2020JC016875)
- 733 Schneider, T., & Griffies, S. M. (1999). A conceptual framework for predictability
734 studies. *Journal of climate*, *12*(10), 3133–3155.
- 735 Schurer, A. P., Hegerl, G. C., Mann, M. E., Tett, S. F., & Phipps, S. J. (2013). Sep-
736 arating forced from chaotic climate variability over the past millennium. *Jour-
737 nal of Climate*, *26*(18), 6954–6973.
- 738 Shannon, C. (1948). A Mathematical Theory of Communication. *Bell System Tech-
739 nical Journal*, *27*(April 1928), 379–423,623–656. Retrieved from [http://math
740 .harvard.edu/~ctm/home/text/others/shannon/entropy/entropy.pdf](http://math.harvard.edu/~ctm/home/text/others/shannon/entropy/entropy.pdf)
- 741 Shchepetkin, A. F., & McWilliams, J. C. (2005). The regional oceanic modeling
742 system (roms): a split-explicit, free-surface, topography-following-coordinate
743 oceanic model. *Ocean modelling*, *9*(4), 347–404.
- 744 Shin, C.-S., Dirmeyer, P. A., & Huang, B. (2023). A joint approach combining corre-

- 745 lation and mutual information to study land and ocean drivers of us droughts:
746 Methodology. *Journal of Climate*, 1–40.
- 747 Stevenson, S., Rajagopalan, B., & Fox-Kemper, B. (2013). Generalized linear mod-
748 eling of the el niño/southern oscillation with application to seasonal forecasting
749 and climate change projections. *Journal of Geophysical Research: Oceans*.
750 Retrieved from <http://dx.doi.org/10.1002/jgrc.20260> (In press)
- 751 Stone, J. V. (2015). *Information theory: a tutorial introduction*. Sebtel Press.
- 752 Timmermans, M.-L., & Jayne, S. R. (2016). The arctic ocean spices up. *Journal of*
753 *Physical Oceanography*, 46(4), 1277–1284.
- 754 Waldman, R., Somot, S., Herrmann, M., Sevault, F., & Isachsen, P. E. (2018). On
755 the chaotic variability of deep convection in the mediterranean sea. *Geophysi-*
756 *cal Research Letters*, 45(5), 2433–2443.
- 757 Watanabe, S. (1960). Information theoretical analysis of multivariate corre-
758 lation. *IBM Journal of Research and Development*, 4(1), 66-82. doi:
759 10.1147/rd.41.0066
- 760 Yettella, V., Weiss, J. B., Kay, J. E., & Pendergrass, A. G. (2018). An ensemble
761 covariance framework for quantifying forced climate variability and its time of
762 emergence. *Journal of Climate*, 31(10), 4117–4133.